

20th International Workshop on
Water Waves and Floating Bodies.
Spitzbergen, 2005.

The Prediction of Viscous Damping of Large Floating Bodies in Waves.

JMR Graham, SJ Sherwin and TE Kendon
Department of Aeronautics, Imperial College, London, UK
and MJ Downie
Department of Marine Technology, University of Newcastle, UK

This contribution will present analysis and results of a method of predicting the contribution to hydrodynamic damping due to flow separation. Normally viscous forces need only be considered when predicting hydrodynamic loading in cases where the relevant Keulegan-Carpenter number is much greater than one. Wave breaking limits these cases to ‘small’ bodies which by definition are not in the diffraction regime. However it is well established that for certain body motions the viscous component of the damping although small relative to the inertia forces is very significant in determining the response amplitude and in fact may be dominant. The most well known case is that of roll damping of ship or barge hulls in beam waves. Other important cases also occur. Examples are slow drift motions in sway and in surge and damping of enclosed fluid in moonpools.

Viscous damping arises from both direct boundary layer effects (skin friction and displacement) and also from the effects of flow separation on the pressure distribution. The direct boundary layer effects are normally negligible at full scale but may be important in model tests. Flow separation usually occurs in cross-flows about local regions of high curvature on the body surface such as the bilges. For sufficiently sharp edges (right angles, bilge keels) the separated flow is essentially independent of the Reynolds number and an inviscid treatment is possible, but if the edges are rounded a viscous treatment is required.

Navier-Stokes computations have been carried out for whole flow fields of this type including the free surface (eg. 1, 2). A disadvantage of a full Navier-Stokes free surface field computation is the large field which must be simulated covering several wavelengths of the incident waves for a satisfactory representation which minimises the effects of the outer boundaries (see eg. discussion in 3). The present method which will be described in this contribution takes advantage of Green’s function methods as typically used for wave potential flows for the dominant part of the flow field. These methods impose the correct outer radiation conditions through the choice of Green’s function without the need to consider any finite outer boundary. The viscous part of the calculation can then be limited to a smaller inner flow field. The method described here [referred to as VISCOR] is designed to be applied as an ‘add-on’ subprogramme to established panel codes based on use of Green’s function and used by the offshore industry.

The basis of VISCOR is the embedding of an inner viscous flow field within the outer potential flow following a Helmholtz split of the velocity field. It is convenient to consider the case of non-steep waves such that

$$H(\text{waveheight})/L(\text{wavelength}) \equiv \varepsilon \ll 1$$

The body length scale b is assumed to be $O(L)$ so that the body is ‘large’ with respect to the wave field and therefore in the diffraction regime. The response amplitude due

to the waves is $O(H)$ and it is assumed that the body has regions of small radius R of curvature (eg. the bilges) where $R = O(H)$ at most and for sharp edges $R \ll H$. A (non-unique) Helmholtz split of the flow field is made by writing:

$$\underline{U}(x, t) = \nabla\phi + \underline{U}_r \quad (1)$$

The potential flow field ϕ is obtained from any Green's function method for the incident, diffracted and radiated fields satisfying zero normal velocity relative to the body surface for all the degrees of freedom in which the body responds. In the present cases the code WAMIT (WAMIT Inc.) because of its high order surface velocity specification was used to provide the linearised, frequency domain, wave potential. This outer flow drives an inner rotational flow field \underline{U}_r satisfying modified Navier-Stokes equations:

$$\frac{\partial \underline{U}_r}{\partial t} + \underline{U} \cdot \nabla \underline{U} = -\frac{1}{\rho} \nabla p + \nu \nabla^2 \underline{U}_r \quad (2)$$

with boundary conditions on the body surface ($\underline{n}, \underline{s}$):

$$\begin{aligned} \underline{U}_r \cdot \underline{n} &= 0 && \text{to satisfy zero normal velocity and} \\ \underline{U}_r \cdot \underline{s} &= -\partial\phi/\partial s && \text{to remove the outer flow slip velocity.} \end{aligned}$$

The spectral-element code Nektar (4) was used to compute the rotational flow field. The rotational flow field occupies a region $O(H)$ in scale around the body and therefore a more limited mesh may be used to compute this part of the flow. To this approximation the inner flow field is local to the body and relatively weak overall. It is therefore appropriate to apply a simple rigid lid boundary condition for \underline{U}_r on the mean free surface and neglect any $O(\epsilon)$ far field waves radiated by the viscous flow field.

VISCOR first computes the potential flow and the body response amplitudes as usual, reconstructing the potential flow field in the time domain over the rotational field mesh. This is then used to compute the rotational flow field in the time domain. The combined force on the body is then input into the matrix equation for the body dynamics (generally for all 6 degrees of freedom, but only 2, sway and roll, in the present case). The response amplitudes are recomputed and the whole procedure iterated to convergence which is rapid (three or four iterations).

In the cases presented here for transverse degrees of freedom, limited to roll and sway, of a long body such as a ship hull (length = b) in beam waves a further approximation can be made, since $H/b = O(\epsilon)$. The rotational flow field computations are carried out on a series of two-dimensional sections (ie. as a strip theory) along the hull, see figure 1 giving further savings in computer time.

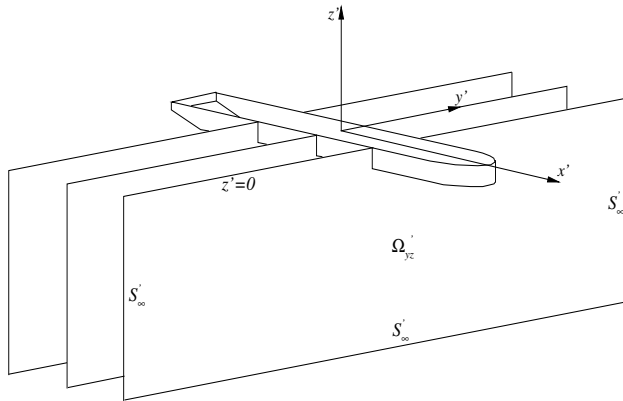


Figure 1. 2-D hull sections.

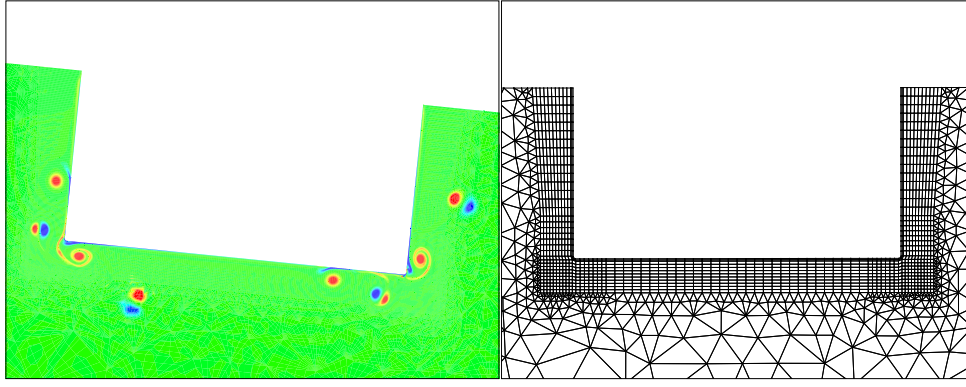


Figure 2. (a) Vortex shedding from section with sharp bilges. (b) Mesh.

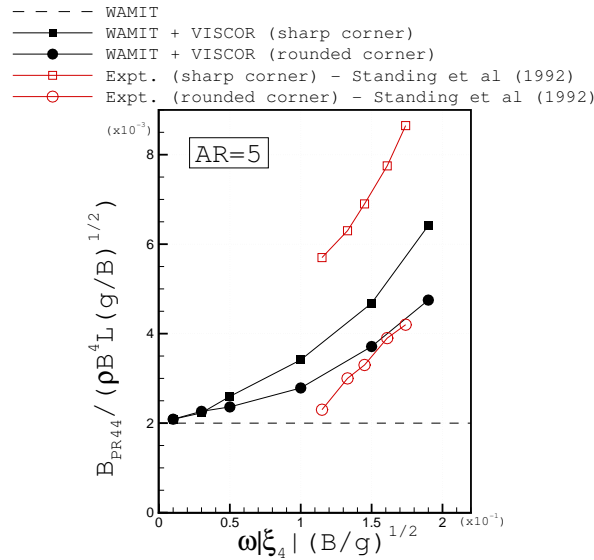


Figure 3 Roll damping coefficient (forced roll) compared with ref.6 experiment.

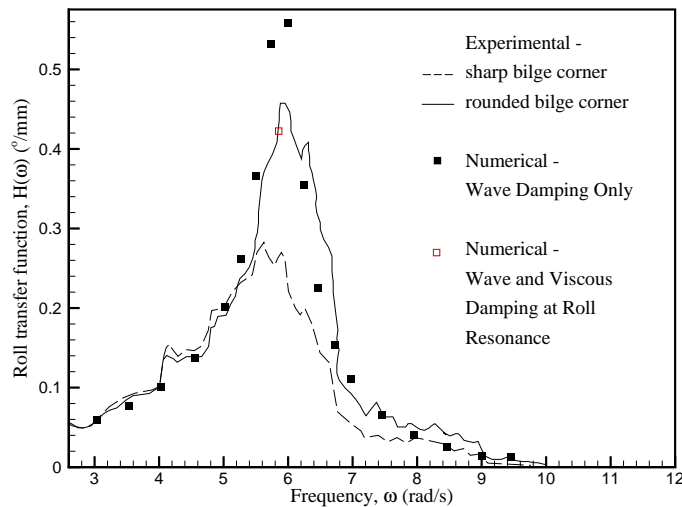


Figure 4 Roll RAO. (free roll and sway) compared with ref. 7 experiment.

After basic validation of VISCOR against a full Navier-Stokes free-surface method (5) for a range of laminar flow problems including two-dimensional flow around a submerged circular cylinder in waves, the code was used to predict hydrodynamic forces on representative hull shapes.

Figure 2 shows the flow field and the mesh used for the rotational flow part of the computation, for a sharp edged hull section in two-dimensional incident waves.

Figure 3 shows comparisons for forced roll around a two-dimensional section with experimental results measured on a model hull spanning a wave flume and forced to roll about a fixed axis close to the mean free surface. Two sets of results are shown for a fixed frequency of oscillation and a range of amplitudes. In the first case the barge had sharp right-angle bilge edges and in the second cases the bilges were rounded. The numerical simulation agrees well with the measured data for the rounded bilge case but under-predicts the roll damping for the sharp edged case.

Figure 4 shows comparisons for a three-dimensional finite length freely floating barge in incident waves. A single numerical result is shown for a frequency close to the roll resonance of a sharp edged hull compared with measurements taken in random seas for the same barge geometry fitted with sharp bilges in one case and rounded bilges in the other. The numerical results under-predict the roll RAO for the sharp bilge case indicating an over-prediction of the damping compared with the experiment. These results and some others (eg. 8) will be discussed in the presentation.

VISCOR computes the rotational flow using the primitive variable formulation of the Navier-Stokes equations. However for rotational flows restricted to two-dimensional sectional computations it is possible to couple the same outer potential flow field to a vorticity based method for the inner rotational flow which solves instead the two-dimensional vorticity transport (curl) form of equation 2:

$$\frac{\partial \omega}{\partial t} + \underline{U} \cdot \nabla \omega = \nu \nabla^2 \omega \quad (3)$$

This equivalent approach was adopted in ref. 9 for prediction of slow drift damping. The present contribution shows results for computations at fairly low Reynolds numbers, usually below those of the experimental data. Laminar flow is assumed, although turbulence modelling based on LES is implemented in the code. If the bilges are sharp and the flow at high enough Reynolds number, the alternative of inviscid analysis is sufficiently accurate. Previous work (10) computed inviscid roll damping coefficients due to separated flow at sharp bilges using a discrete vortex approach which solves in principle the inviscid two-dimensional form of equation 3. This work additionally used an edge matching procedure which effectively allowed the relatively expensive computation of the rotational flow to be pre-calculated and stored for all cases. Results of this method and comparisons with VISCOR will also be discussed.

References.

- 1 Yeung, R. and Vaidhyanathan, M. 1994 Proc. Int. Conf. Hydro., Wuxi, China
- 2 Robertson, I., Graham M., Sherwin, S. and Kendon, T. 2002 AMIF Conf. Lisbon.
- 3 Ferrant P, Gentaz L, Alessandrini B and Le Touze D. 2003 Ship Tech Res. 50.
- 4 Sherwin SJ. and Karniadakis GM. 1995 Int. Conf. F.E. in Fluids, Venice.
- 5 Kendon, TE., Sherwin, SJ. and Graham JMR. 2003 2nd MIT Conf. Comp FSM
- 6 Standing, RG., Jackson, GE. and Brook, AK. 1992 Proc. BOSS 92, London.
- 7 Brown, DT., Eatock Taylor, R. and Patel, MH. 1983 J.Fluid Mech. 129, p385
- 8 Vugts, J. 1968 Int. Shipbuilding Progress, p 251.
- 9 Graham, JMR. and Neish, A. 1996 Proj. B2 Rept. ULOS Prog. MTD London.
- 10 Downie MJ., Bearman PW. and Graham JMR. 1988 J. Fluid Mech. 189, p243